

Prediction of stable $C_{7/12}$ and metastable $C_{4/7}$ commensurate solid phases for ^4He on graphite

Jeonghwan Ahn, Hoonkyung Lee, and Yongkyung Kwon*

Division of Quantum Phases and Devices, School of Physics, Konkuk University, Seoul 143-701, Korea

(Received 28 April 2015; revised manuscript received 28 August 2015; published 17 February 2016)

Using a substrate potential described by a pairwise sum of empirical ^4He -C interatomic potentials, we have performed path-integral Monte Carlo calculations for ^4He adatoms on graphite. It is found that a second-layer commensurate structure is not stable above an incommensurate first-layer triangular solid. This is consistent with the conclusion of the previous theoretical study of Corboz *et al.* [*Phys. Rev. B* **78**, 245414 (2008)] that was based on a laterally averaged one-dimensional potential. On the other hand, we observe a new stable $C_{7/12}$ commensurate solid in the first ^4He layer at the areal density of 0.111 \AA^{-2} , which is close to the second-layer promotion density. This high-density commensurate solid exhibits a $\sqrt{12} \times \sqrt{12}$ structure registered to the graphite surface that is not disrupted by the development of the second ^4He layer. Furthermore, a second-layer $4/7$ commensurate structure relative to the first-layer $C_{7/12}$ solid is found to be at least metastable, opening the possibility of two-dimensional supersolidity.

DOI: [10.1103/PhysRevB.93.064511](https://doi.org/10.1103/PhysRevB.93.064511)

The ^4He adsorption on an extended flat substrate of graphite has been under intensive studies for the past few decades. The strong attraction by the substrate allows helium adatoms to form multiple distinct two-dimensional (2D) layers on graphite [1]. Due to the interplay between ^4He - ^4He interactions and ^4He -substrate interactions, these helium layers exhibit rich structural phase diagrams. It is well established that the monolayer of ^4He atoms on graphite undergoes a transition from a $C_{1/3}$ commensurate solid at the areal density of 0.0636 \AA^{-2} to an incommensurate solid as the helium coverage increases. Based on the observation of the melting peaks in the heat capacity data, Greywall and Busch proposed a phase diagram of the first ^4He layer including another commensurate structure at a high areal density just before entering the incommensurate solid region [2]. For the second ^4He layer, Greywall observed the heat capacity peaks to signal a commensurate solid structure at the helium coverages between a low-density liquid phase and a high-density incommensurate solid phase [3], which was thought to be a $C_{4/7}$ structure with respect to a first-layer incommensurate triangular solid. On the other hand, using torsional oscillator experiments, Crowell and Reppy first observed finite superfluid fractions in the second ^4He layer [4]. The period shifts in their experiments were observed at the helium coverages extended into the commensurate density region claimed by Greywall, which prompted early speculation of possible 2D supersolidity [5].

On theoretical sides, path-integral Monte Carlo (PIMC) calculations of Pierce and Manousakis [6] showed that the ^4He monolayer on graphite possessed solid clusters and was not in a superfluid phase at low helium coverages below the $C_{1/3}$ commensurate density. Based on their own PIMC calculations, Corboz *et al.* [7] later proposed a full phase diagram of the ^4He monolayer, confirming the commensurate-incommensurate transition with the increase in the helium coverage. They also observed a new $C_{7/16}$ commensurate solid at the areal density of 0.0835 \AA^{-2} , which was speculated to be the high-density commensurate phase Greywall and

Busch [2] identified from their heat capacity measurements. On the other hand, Gordillo and Boronat performed diffusion Monte Carlo (DMC) calculations to predict that a low-density liquid phase could be realized, at least metastably, in the ^4He monolayer on graphene [8]. Furthermore, subsequent DMC study of Gordillo *et al.* showed the activation of mobile vacancies in the $C_{1/3}$ commensurate solid on graphene or graphite to induce a 2D supersolidity [9]. For the second ^4He layer on graphite, the PIMC study of Pierce and Manousakis predicted a stable $4/7$ commensurate structure above a frozen first-layer incommensurate triangular solid [10,11]. However, the PIMC calculations of Corboz *et al.* [7] revealed that no commensurate solid phase would be stable on top of a first-layer incommensurate solid when zero-point motions of the first-layer ^4He atoms were fully incorporated. This led them to propose a theoretical phase diagram of the second ^4He layer involving a direct transition from a superfluid phase to an incommensurate solid without experiencing a commensurate solid phase. No stable second-layer commensurate structure was also reported in recent theoretical studies for the ^4He adsorption on graphene [12–14]. Contrary to the conclusion drawn from these theoretical studies, however, Nakamura *et al.* recently reported an experimental observation of indicating a commensurate solid phase in the second ^4He layer, which was based on their new heat capacity measurements for ^4He on a ZYX exfoliated graphite substrate [15].

As described above, the existence of a stable commensurate solid phase in the second ^4He layer on graphite is still under debate. Noting that a laterally averaged one-dimensional (1D) substrate potential was used in all previous PIMC studies for the second ^4He layer, we have decided to perform new PIMC calculations with an anisotropic ^4He -graphite potential reflecting the surface corrugation. The use of the 1D potential was justified by the fact that the lateral variations of the substrate interaction should be minimal for the second-layer ^4He atoms located far enough ($\sim 5.7 \text{ \AA}$) from the graphite surface. However, the PIMC calculations of Corboz *et al.* showed that the inclusion of zero-point motions of the first-layer ^4He atoms destabilized, otherwise stable, a second-layer commensurate solid phase, suggesting that quantum dynamics of the first helium layer could affect the second-layer phase diagram. Our

*ykwon@konkuk.ac.kr

PIMC calculations with a corrugated substrate potential are expected to make a more accurate description of quantum dynamics of the first-layer ^4He atoms and to lead to a more definite conclusion for the second-layer phase diagram. We find that a presumed $C_{4/7}$ commensurate phase of the second ^4He layer is unstable above a first-layer incommensurate solid even under our corrugated substrate potential. On the other hand, we have found a new stable commensurate solid in the first ^4He layer at a high areal density of 0.111 \AA^{-2} . This newly found high-density commensurate phase, which has a $C_{7/12}$ structure with respect to the underlying graphite surface, is not disturbed by the adsorption of additional ^4He atoms and its structure is preserved with the development of the second ^4He layer. Furthermore, we find that the ^4He configuration of a second-layer $4/7$ commensurate structure on top of a first-layer $C_{7/12}$ solid is at least metastable.

In this study, the ^4He -graphite interaction is described by a sum of interatomic pair potentials between the carbon atoms in the topmost layer of graphite and a ^4He atom plus the 1D potential coming from the rest of the carbon layers:

$$V_{\text{He-graphite}} = \sum_i^{\text{topmost}} V_{\text{He-C}}(\vec{r} - \vec{r}_i) + V_{\text{1D}}(z + 3.35 \text{ \AA}). \quad (1)$$

For the ^4He -C interatomic pair potential $V_{\text{He-C}}$, we use an anisotropic 6-12 Lennard-Jones potential, which was proposed by Carlos and Cole to fit helium scattering data from graphite surfaces [16,17]. And the laterally averaged 1D potential V_{1D} is the same as the one used in previous PIMC studies for the second ^4He layer [7,10,11] (note that the interlayer spacing of graphite is 3.35 \AA). A well-known Aziz potential [18] is used for the ^4He - ^4He interaction. In the path-integral representation, the thermal density matrix at a low temperature T is expressed as a convolution of M high-temperature density matrices with an imaginary time step $\tau = (Mk_B T)^{-1}$. While the anisotropic part of the ^4He -C pair potential is treated with the primitive approximation, the ^4He - ^4He potential, the isotropic part of ^4He -C interatomic potential, and the 1D substrate potential V_{1D} are used to compute the exact two-body density matrices [19,20] at the high temperature MT . This was found to provide an accurate description of the ^4He -substrate interaction as well as the ^4He - ^4He interaction with a time step of $\tau^{-1}/k_B = 80 \text{ K}$. Periodic boundary conditions with a fixed rectangular simulation cell are used along the lateral directions to minimize finite size effects while no boundary condition is assumed in the vertical direction.

With the ^4He -substrate potential described above, we first performed PIMC calculations for the second-layer ^4He atoms adsorbed above a first-layer incommensurate solid. Our simulation cell for these calculations is a 6×11 rectangular cell with dimensions of $25.56 \times 27.05 \text{ \AA}^2$. The simulations started from an initial configuration of 84 ^4He atoms located at predetermined triangular lattice sites of the first layer along with additional 48 ^4He atoms distributed randomly at the distances far from the graphite surface, which leads to the first-layer and the second-layer areal densities of 0.121 and 0.0694 \AA^{-2} . Note that this first-layer areal density is in the density range of 0.115 to 0.127 \AA^{-2} [2,7,21] reported previously for the completed first

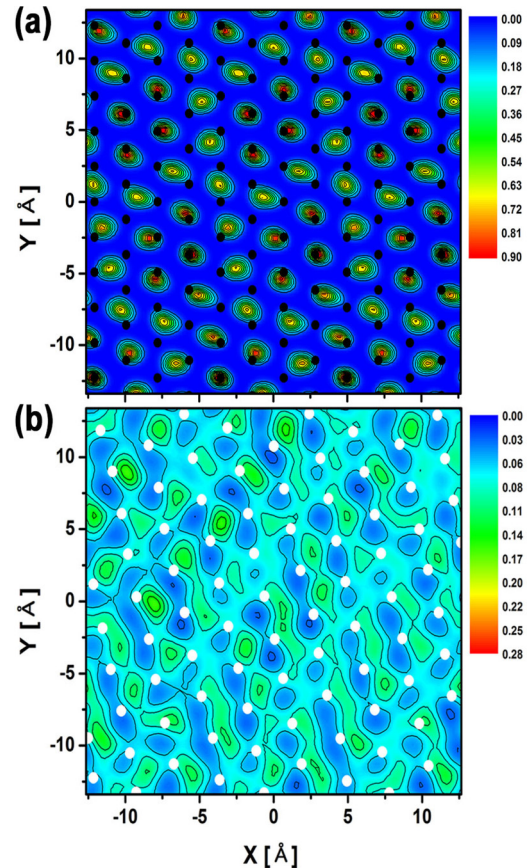


FIG. 1. Contour plots of two-dimensional density distributions of (a) the first-layer and (b) the second-layer ^4He atoms (red: high density, blue: low density). The computations were done at $T = 0.5 \text{ K}$ with the 6×11 rectangular simulation cell which involves 84 first-layer ^4He atoms constituting an incommensurate triangular solid and 48 additional ^4He atoms forming the second layer. While the black dots in (a) correspond to the adsorption sites (the hexagon centers) on the graphite surface, the white dots in (b) represent the peak positions of the first-layer ^4He density distribution.

^4He layer and our second-layer density is set to simulate the $4/7$ commensurate phase relative to the first-layer triangular solid. The equilibrated 2D density distribution of the first-layer ^4He atoms is shown in Fig. 1(a), which demonstrates 84 clear density peaks constituting a triangular lattice not commensurate with the underlying surface structure of graphite. The 2D density distribution of the second ^4He layer is presented in Fig. 1(b). Here the white dots represent the peak positions of the first-layer helium density distribution of Fig. 1(a). In these computations, both quantum dynamics and quantum statistics of all ^4He atoms, including the first-layer ^4He atoms, were fully incorporated. As seen in Fig. 1(b), the second ^4He layer does not show any crystalline order but is in a fluid state. Our PIMC calculations with a corrugated substrate potential lead to the same conclusion as the previous calculations of Corboz *et al.* [7] based on a laterally averaged 1D potential; a presumed $4/7$ commensurate structure of the second-layer ^4He atoms is not stable above a first-layer incommensurate solid.

From further investigation of the ^4He adsorption on graphite, we could confirm the existence of the first-layer $C_{7/16}$

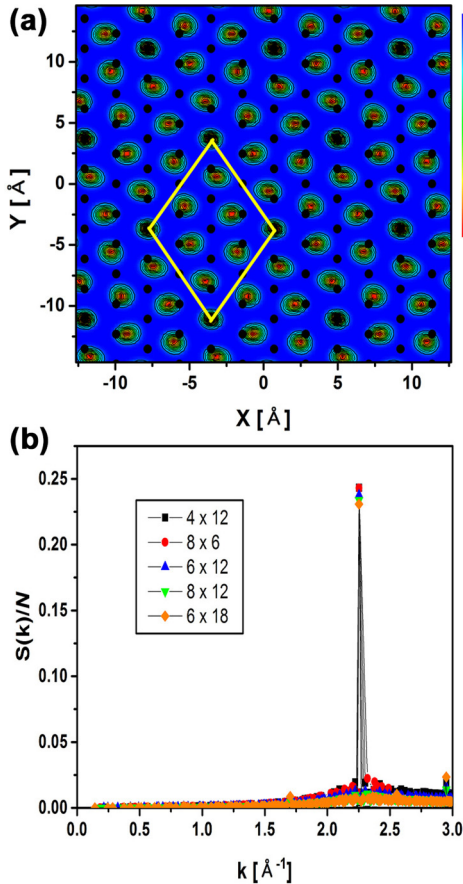


FIG. 2. (a) Two-dimensional density distribution of the ^4He monolayer at an areal density of 0.111 \AA^{-2} (red: high density, blue: low density) and (b) its static structure factor divided by the number of ^4He atoms as a function of wave vector k . The computations were done at a temperature of 0.5 K. While the black dots in (a) represent the adsorption sites on the graphite surface, the black, red, blue, green, and orange symbols in (b) represent the PIMC data for the 4×12 , 8×6 , 6×12 , 8×12 , and 6×18 rectangular simulation cells, respectively. The statistical errors are smaller than the symbol sizes.

commensurate phase that was first reported by Corboz *et al.* [7]. In addition, we find a new high-density commensurate structure in the first ^4He layer at the areal density of 0.111 \AA^{-2} . The 2D density distribution of Fig. 2(a) shows the well-distinct density peaks to constitute a triangular lattice. This corresponds to a $C_{7/12}$ commensurate solid, or a $\sqrt{12} \times \sqrt{12}$ registered structure, with respect to the graphite surface, as evidenced by a rhombic unit cell represented by yellow lines involving 7 ^4He atoms and 12 adsorption sites. Unlike those for an incommensurate solid structure shown in Fig. 1(a), these simulations started from an initial configuration of ^4He atoms in a gas phase which were randomly distributed at the distances far away from the graphite surface, suggesting that this is a thermodynamically stable structure at the corresponding helium density. To confirm the formation of this commensurate structure we compute the static structure factors divided by the number of ^4He atoms using five different simulation cells, which are presented in Fig. 2(b) as functions of wave vector k .

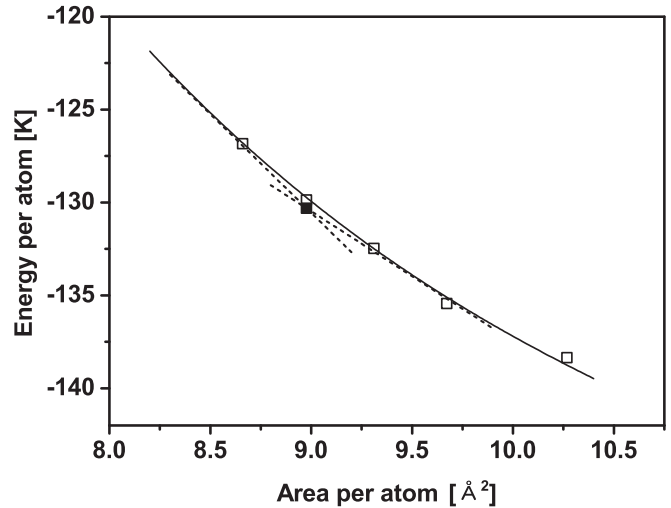


FIG. 3. Energy of the first-layer ^4He atoms on graphite as a function of the inverse of the helium density for the incommensurate triangular solid phase (open squares) and for the $C_{7/12}$ commensurate solid (solid square). The computations were done at a temperature of 0.5 K. The statistical errors are smaller than the symbol sizes. The solid curve is a third-order polynomial fit to the incommensurate energies and the dotted lines represent a Maxwell construction between the two different solid phases.

The peaks are observed at the reciprocal primitive vectors corresponding to the $7/12$ commensurate solid, whose magnitude is 2.25 \AA^{-1} , for all system sizes. Little difference among the peak values for different system sizes says that the structural features of the $C_{7/12}$ commensurate solid are not affected by the finite sizes of our systems. We have also found that the energy per ^4He atom changes very little, less than 0.1 K/atom , as the size of the simulation cell varies, reflecting the short-ranged nature of both ^4He - ^4He and ^4He -C interactions. In addition, the same $C_{7/12}$ commensurate structure was observed to form under the ^4He -graphite potential that Pierce and Manousakis [6] and Corboz *et al.* [7] used in their PIMC calculations, a Fourier series expansion in the reciprocal lattice vectors of the graphite substrate [16]. This suggests that the formation of this new commensurate structure is not a consequence of our treatment of the ^4He -graphite interaction.

Another confirmation of the stable $C_{7/12}$ commensurate solid comes from an energetic analysis of the ^4He monolayer at high helium coverages. Figure 3 shows the energy per ^4He atom computed at $T = 0.5 \text{ K}$, as a function of the inverse of the areal density, where the open symbols represent the energies of the incommensurate triangular solids at the respective densities and the solid symbol corresponds to the energy of the $C_{7/12}$ commensurate solid. The zero-temperature energies are expected to be about the same as the ones presented here because we observe little difference between the PIMC energies at $T = 0.25 \text{ K}$ and those at 0.5 K . One can see that the total energy of the $C_{7/12}$ commensurate solid is lower by $\sim 0.5 \text{ K/atom}$ than that of an incommensurate solid at the same density, indicating that the former could be energetically more stable, albeit slightly, than the latter. Furthermore, the high-density phase diagram of the first ^4He layer on graphite can be established by a double-tangent Maxwell construction with

Fig. 3. Since the homogeneous $C_{7/12}$ phase is defined by the single density of 0.111 \AA^{-2} , or at the surface area of 8.98 \AA^2 per atom, and should be in equilibrium with the incommensurate triangular solid, the density range for the phase coexistence is determined by drawing the tangent lines to the equation of state of the incommensurate solid phase that pass through the $7/12$ commensurate point [8,22,23] (see the dotted lines in Fig. 3). From this, the phase boundaries are estimated to be 0.104 and 0.118 \AA^{-2} , between which we expect the $C_{7/12}$ commensurate structure to coexist with the incommensurate solid. Little energy difference between the two phases in this regime could be the reason why the $C_{7/12}$ commensurate phase has not been experimentally identified yet.

We note that the $C_{7/12}$ commensurate density is inside the density range identified as the incommensurate solid regime and is very close to the second-layer promotion densities reported in the previous experimental and theoretical studies [7,21,24–27]. Among others, neutron scattering experiment of Lauter *et al.* [28] showed diffraction peaks at $Q \simeq 2.26 \text{ \AA}^{-1}$, the reciprocal primitive vector of a triangular solid at the density of 0.112 \AA^{-2} , beyond which the ^4He atoms were promoted to the second layer. From the fact that the observed second-layer promotion density is nearly identical to the $C_{7/12}$ commensurate density, one can speculate that the second ^4He layer could be developed on top of the first-layer $C_{7/12}$ commensurate structure. This leads us to perform additional ^4He adsorption on a first-layer $C_{7/12}$ solid. Figure 4(a) shows 1D ^4He density distribution for the adsorption of additional 48 ^4He atoms per 6×12 simulation cell, which were initially located at the distances far from the first-layer $C_{7/12}$ solid. It is found that the first-layer density peak changes very little and all additional ^4He atoms form the second layer without squeezing into the first layer, from which the first-layer $C_{7/12}$ structure is expected to be preserved with additional ^4He adsorption. This suggests that the configuration of the second-layer ^4He atoms plus the first-layer $C_{7/12}$ solid corresponds to at least a local minimum. We now analyze the structure of the second helium layer in this configuration, whose 2D density distribution is presented in Fig. 4(b). While the white dots representing the peak positions of the first-layer ^4He density distribution confirm the first-layer $C_{7/12}$ structure, the second-layer density peaks are also seen to form a triangular lattice. Furthermore, this second-layer lattice is commensurate with the underlying first-layer triangular lattice; a rhombic unit cell enclosed by yellow lines in Fig. 4(b) includes four second-layer lattice sites and seven first-layer ones. This $4/7$ commensurate structure is registered by $\sqrt{7} \times \sqrt{7}$ to the first-layer triangular lattice. Finally, we have found that structural features of the second-layer $C_{4/7}$ solid are maintained with the formation of vacancy defects. Clear structure-factor peaks are observed at the reciprocal primitive vectors corresponding to the $4/7$ commensurate solid when the vacancies up to 4% of the commensurate lattice sites are created. These vacancies are also found to be mobile as a result of frequent hopping of the second-layer ^4He atoms to the neighboring lattice sites, which implies that a 2D supersolid phase could be realized in the second-layer $4/7$ commensurate solid.

Through the PIMC calculations of using a fully corrugated ^4He -graphite potential, we have investigated the stability of a

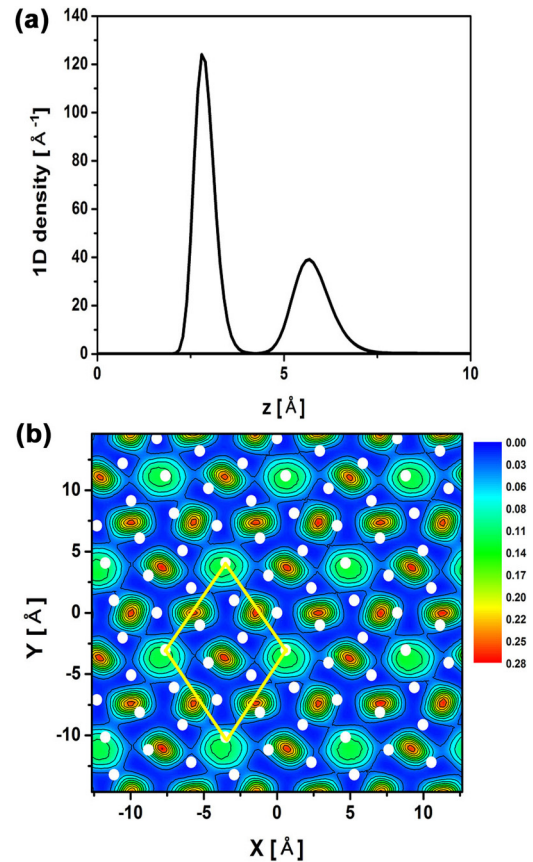


FIG. 4. (a) One-dimensional density of ^4He atoms adsorbed on graphite as a function of the distance z (in \AA) from the graphite surface and (b) two-dimensional density distribution of the second-layer ^4He atoms (red: high density, blue: low density). The computations were done at a temperature of 0.5 K for 48 additional ^4He adatoms per 6×12 rectangular simulation cell on top of the first-layer commensurate structure of Fig. 2(a). The white dots in (b) represent the peak positions of the first-layer ^4He density distribution.

commensurate structure in the second ^4He layer on graphite. The second ^4He layer does not exhibit a stable commensurate structure on top of a first-layer incommensurate solid. This result is consistent with the conclusion of Corboz *et al.* [7] in a sense that zero-point motions of the first-layer ^4He atoms as well as quantum exchanges among ^4He atoms destabilize a second-layer commensurate structure above a first-layer incommensurate solid. On the other hand, we have observed a new stable $C_{7/12}$ commensurate structure in the first ^4He layer at the areal density of 0.111 \AA^{-2} . It is found that additional ^4He adsorption leads to the development of the second layer without disrupting the first-layer commensurate structure and the second-layer ^4He atoms form a commensurate solid at the $4/7$ density relative to the first-layer $C_{7/12}$ commensurate filling. We note that the total helium coverage for a second-layer $C_{4/7}$ solid plus a first-layer $C_{7/12}$ solid is rather low in comparison to those identified in some heat-capacity measurements [3,15] for the second-layer commensurate solid phase. It is generally accepted that the first ^4He layer is an incommensurate solid at its completion with the areal density of 0.115 to 0.127 \AA^{-2} , which is somewhat higher than the $7/12$ commensurate

density we found. From the fact that our PIMC simulations started from a random initial configuration of ^4He atoms located far away from the substrate, however, we conclude that the configuration of a second-layer $4/7$ commensurate structure on top of a first-layer $7/12$ commensurate solid is at least metastable on graphite. Experimentally-observed large heat-capacity anomalies [3,15] might be attributed to the melting of this second-layer commensurate structure. Since the existence of a second-layer commensurate solid is critical

in realizing a supersolid phase in a ^4He -graphite system, this elusive state of matter could emerge as a metastable phase.

This work was supported by Konkuk University. We also acknowledge the support from the Supercomputing Center/Korea Institute of Science and Technology Information with supercomputing resources including technical support (KSC-2015-C3-041).

-
- [1] G. Zimmerli, G. Mistura, and M. H. W. Chan, *Phys. Rev. Lett.* **68**, 60 (1992).
- [2] D. S. Greywall and P. A. Busch, *Phys. Rev. Lett.* **67**, 3535 (1991).
- [3] D. S. Greywall, *Phys. Rev. B* **47**, 309 (1993).
- [4] P. A. Crowell and J. D. Reppy, *Phys. Rev. Lett.* **70**, 3291 (1993).
- [5] P. A. Crowell and J. D. Reppy, *Phys. Rev. B* **53**, 2701 (1996).
- [6] M. E. Pierce and E. Manousakis, *Phys. Rev. Lett.* **83**, 5314 (1999).
- [7] P. Corboz, M. Boninsegni, L. Pollet, and M. Troyer, *Phys. Rev. B* **78**, 245414 (2008).
- [8] M. C. Gordillo and J. Boronat, *Phys. Rev. Lett.* **102**, 085303 (2009).
- [9] M. C. Gordillo, C. Cazorla, and J. Boronat, *Phys. Rev. B* **83**, 121406(R) (2011).
- [10] M. E. Pierce and E. Manousakis, *Phys. Rev. Lett.* **81**, 156 (1998).
- [11] M. E. Pierce and E. Manousakis, *Phys. Rev. B* **59**, 3802 (1999).
- [12] Y. Kwon and D. M. Ceperley, *Phys. Rev. B* **85**, 224501 (2012).
- [13] M. C. Gordillo and J. Boronat, *Phys. Rev. B* **85**, 195457 (2012).
- [14] J. Happacher, P. Corboz, M. Boninsegni, and L. Pollet, *Phys. Rev. B* **87**, 094514 (2013).
- [15] S. Nakamura, K. Matsui, T. Matsui, and H. Fukuyama, [arXiv:1406.4388](https://arxiv.org/abs/1406.4388).
- [16] W. E. Carlos and M. W. Cole, *Surf. Sci.* **91**, 339 (1980).
- [17] M. W. Cole and J. R. Klein, *Surf. Sci.* **124**, 547 (1983).
- [18] R. A. Aziz, M. J. Slaman, A. Koide, A. R. Allnatt, and W. J. Meath, *Mol. Phys.* **77**, 321 (1992).
- [19] D. M. Ceperley, *Rev. Mod. Phys.* **67**, 279 (1995).
- [20] R. E. Zillich, F. Paesani, Y. Kwon, and K. B. Whaley, *J. Chem. Phys.* **123**, 114301 (2005).
- [21] M. Bretz, J. G. Dash, D. C. Hickernell, E. O. McLean, and O. E. Vilches, *Phys. Rev. A* **8**, 1589 (1973).
- [22] M. C. Gordillo and J. Boronat, *Phys. Rev. B* **81**, 155435 (2010).
- [23] C. Carbonell-Coronado and M. C. Gordillo, *Phys. Rev. B* **85**, 155427 (2012).
- [24] K. Carneiro, L. Passell, W. Thomlinson, and H. Taub, *Phys. Rev. B* **24**, 1170 (1981).
- [25] H. J. Lauter, H. P. Schildberg, H. Godfrin, H. Wiechert, and R. Haensel, *Can. J. Phys.* **65**, 1435 (1987).
- [26] S. E. Polanco and M. Bretz, *Phys. Rev. B* **17**, 151 (1978).
- [27] P. A. Whitlock, G. V. Chester, and B. Krishnamachari, *Phys. Rev. B* **58**, 8704 (1998).
- [28] H. J. Lauter, H. Godfrin, V. L. P. Frank, and P. Leiderer, in *Phase Transitions in Surface Films 2*, edited by H. Taub *et al.* (Plenum, New York, 1991), p. 135.